Population trapping: The mechanism for the lost resonance lines in Pm-like ions

Elsevier Editorial System(tm) for NIMB Proceedings

Manuscript Draft

Manuscript Number: NIMB_PROCEEDINGS-D-16-00412R1

Title: Population Trapping: The Mechanism for The Lost Resonance Lines in Pm-like Ions

Article Type: SI: NIMB_HCI 2016

Section/Category: SI: NIMB_HCI 2016

Keywords: alkaline metal-like resonance line; Pm-like ion; meta-stable state; collisional-radiative model; EBIT; EUV spectra

Corresponding Author: Dr. Daiji Kato,

Corresponding Author's Institution: National Institute for Fusion Science

First Author: Daiji Kato

Order of Authors: Daiji Kato; Hiroyuki A Sakaue; Izumi Murakami; Nobuyuki Nakamura

Manuscript Region of Origin: JAPAN

Abstract: We report a population kinetics study on line emissions of the Pm-like Bi^{22+} performed by using a collisional-radiative (CR) model. Population rates of excited levels are analyzed to explain the population trapping in the $4f^{13}\ 5s^2$ state which causes the loss of the 5s-5p resonance lines in emission spectra. Based on the present analysis, we elucidate why the population trapping is not facilitated for a meta-stable excited level of the Sm-like Bi^{21+}. The emission line spectra are calculated for the Pm-like isoelectronic sequence from Au^{18+} through W^{13+} and compared with experimental measurements by electron-beam-ion-traps (EBITs). Structures of the spectra are similar for all of the cases except for calculated W^{13+} spectra. The calculated spectra are hardly reconciled with the measured W^{13+} spectrum using the compact electron-beam-ion-trap (CoBIT) [Phys. Rev. A 92 (2015) 022510].

Population Trapping: The Mechanism for The Lost Resonance Lines in Pm-like Ions

Daiji Kato[a,b], Hiroyuki A. Sakaue[a], Izumi Murakami[a,b], and Nobuyuki Nakamura[c]

[a]*National Institute for Fusion Science, Gifu 509-5292, Japan*

[b]*Dept. of Fusion Science, SOKENDAI (The Graduate University for Advanced Studies), Gifu 509-5292, Japan*

[c]*Inst. for Laser Science, The Univ. of Electro-Communications, Tokyo 182-8585, Japan*

Abstract

We report a population kinetics study on line emissions of the Pm-like Bi^{22+} performed by using a collisional-radiative (CR) model. Population rates of excited levels are analyzed to explain the population trapping in the $4f^{13}5s^2$ state which causes the loss of the $5s-5p$ resonance lines in emission spectra. Based on the present analysis, we elucidate why the population trapping is not facilitated for a meta-stable excited level of the Sm-like Bi^{21+}. The emission line spectra are calculated for the Pm-like isoelectronic sequence from Au^{18+} through W^{13+} and compared with experimental measurements by electron-beam-ion-traps (EBITs). Structures of the spectra are similar for all of the cases except for calculated W^{13+} spectra. The calculated spectra are hardly reconciled with the measured W^{13+} spectrum using the compact electron-beam-ion-trap (CoBIT) [Phys. Rev. A 92 (2015) 022510].

Keywords: alkaline metal-like resonance line; Pm-like ion; meta-stable state; collisional-radiative model; EBIT; EUV spectra

1. Introduction

Promethium (Pm) has the $4f$ electron shell which is a loosely bound outermost orbital in a screened nuclear field. As the atomic number (Z) increases along the Pm isoelectronic sequence, the $4f$ orbital energy falls beneath the $5s$ orbital energy as in the hydrogenic system (orbital collapse) because screening of nuclear fields by ambient electrons in atomic systems becomes less significant for highly charged ions. Curtis and Ellis [1] in their pioneering work based on Hartree-Fock calculations predicted that the Pm sequence has the alkaline metal-like ground configuration: $4f^{14}5s$ for heavier elements of $Z > 73$ and should exhibit strong $5s - np$ resonance line emissions in hot plasmas. Follow-up studies by fully relativistic Dirac-Fock calculations [2], multireference Møller-Plesset second-order perturbation calculations [3], and relativistic many-body perturbation calculations [4] predicted that the cross-over of $4f^{13}5s^2$ and $4f^{14}5s$ levels will occur in between Z =77 and 78.

Wavelengths of the $5s - 5p$ resonance lines are predicted to fall in extreme ultra-violet (EUV) and soft X-ray regions (8 – 38 nm) for $Z = 74 - 92$. In spite of many experimental [5-10] and theoretical [11,12] works devoted to seeking for the resonance lines in emission spectra of heavy elements, there has yet to be a definite identification of the predicted resonance lines. Recently, Kobayashi et al. [13] reported that any prominent line of Pm-like Bi^{22+} ($Z = 83$) ions in the compact electron-beam-ion-trap (CoBIT) [14] is not identified as the $4f^{14}5s - 4f^{14}5p$ transitions but as the $4f^{13}5s^2 - 4f^{13}5s5p$ transitions, although the ground state configuration is $4f^{14}5s$ as predicted by theories. This experimental observation is explained by population trapping in a long-lived excited level of the $4f^{13}5s^2$ at electron densities in CoBIT (estimated to be about 10^{10} cm^{-3}). Bekker et al. [15] and Kobayashi et al. [16] studied emission spectra of the Pm-like ions in EBITs for elements from Pm-like Pt^{17+} (78) through Re^{14+} (75) and Bi^{22+}, Au^{18+} (79), and W^{13+} (74), respectively. While they observed weak $5s - 5p_{3/2}$ resonance lines in the spectra except for tungsten, the emission spectra for all of the elements they studied are dominated by the $4f^{13}5s^2 - 4f^{13}5s5p$

transitions. Li et al. [17] assigned other Pm-like lines prominent in tungsten spectra measured by high-temperature superconducting EBIT (SH-HtscEBIT) to $4f^{12}5s^25p - 4f^{12}5s5p^2$ and $4f^{12}5s^25p - 4f^{12}5s^25d$ transitions. However, the assignment is inconsistent with that by Kobayashi et al. [16].

In the present paper, we report a population kinetics study on line emissions of the Pm sequence performed by using a collisional-radiative (CR) model. Population rates of excited levels are analyzed to explain the population trapping in the $4f^{13}5s^2$ state which causes the loss of the $5s - 5p$ resonance lines in emission spectra. Problematic Pm-like tungsten spectra are studied in detail.

2. Theoretical model

Emission line intensities are expressed by products of intrinsic transition probabilities and populations of ions in excited-states. The populations are calculated by a kinetics model called the collisional-radiative (CR) model. In the CR model, it is assumed that the excited-state population is in a steady-state at given rates of (de)excitation and ionization of the ions bombarded by a mono-energetic electron beam of the EBIT and subsequent radiative decays. Recombination (radiative and dielectronic) and charge exchange processes are neglected at all in the present model. The populations of an excited-state i (n_i) are solutions of the following equilibrium equation,

$$n_{\mathrm{e}} \sum_{j \neq i} C_{ij} n_j + \sum_{j>i} A_{ij} n_j = \left(n_{\mathrm{e}} \sum_{j \neq i} C_{ji} + \sum_{j<i} A_{ji} \right) n_i, \tag{1}$$

where C_{ij} are electron collision rate coefficients, A_{ij} radiative transition rates, and n_{e} electron densities. The first and the second terms of the left-hand side are in-flow rates of populations to the excited-state i due to collisional (de)excitation and radiative cascade from higher excited-states, respectively. On the other hand, the first and the second terms of the right-hand

side stand for out-flow rates from the excited-state due to the collisional (de)excitation and ionization and radiative decay to lower states, respectively. Eq. (1) is solved for the excited-states with a given population of the ground-state as $n_0 = 1$, and then the solutions are renormalized to be $\sum_{i=0} n_i = 1$.

Energy levels of $4f^{14}nl\ (n = 5,6; l = 0-4)$, $4f^{13}\{5snl, 5p^2, 5p5l, 5d^2\}$, $4f^{12}\{5s^25l, 5s5p^2\}$, and $4f^{11}5s^25p^2$ (2285 levels in total) and those of $4f^{14}\{5snl, 5p^2, 5p5l, 5d^2\}$, $4f^{13}\{5s^25l, 5s5p^2\}$, and $4f^{12}5s^25p^2$ (492 levels in total) are taken into account for Pm-like and Sm-like ions, respectively. The energy levels, radiative transition probabilities (electric-dipole, quadruple and octupole, and magnetic-dipole and quadruple), and distorted-wave electron-collision cross sections are calculated with fully relativistic wave-functions obtained by optimized parametric radial potentials. These calculations are implemented using HULLAC code (v9.601) [18].

3. Results and discussion

Figure 1 shows emission line spectra of Pm-like Bi^{22+} and Sm-like Bi^{21+} ions in CoBIT measured by Kobayashi et al. [13, 16] compared with those obtained by the present calculations. The electron density is typically estimated to be about 10^{10} cm^{-3}, which is used for the present calculations. The experimental spectra are shown for three electron beam energies of 500, 580, and 640 eV, respectively. Two emission lines observed at 14.3 and 26.2 nm in the spectrum for 580 eV are absent in the spectrum for 500 eV. Since the ionization energies of the Eu-like Bi^{20+} and the Sm-like Bi^{21+} are 548 eV and 621 eV [19] (608.8 eV, present calculation), respectively, these two lines are assigned to the Bi^{21+}. Similarly, five lines at 13.8, 14.0, 25.7, 25.9, and 26.0 nm in the spectrum for 640 eV which is above the ionization energy of the Sm-like Bi^{21+} are assigned to the Pm-like Bi^{22+}. The ionization energy of the Bi^{22+} is 659 eV [19] (639.0 eV, present calculation). It is noted that the electron beam energy in CoBIT can have a width of about 5 eV. Based on the calculated spectra, the Pm-like

line at 13.8 nm is identified as a blend of $4f_{7/2}^{-1}5s^2 - \left[4f_{7/2}^{-1}5s5p_{3/2}\right]_{7/2}$ and $4f_{5/2}^{-1}5s^2 - \left[4f_{5/2}^{-1}5s5p_{3/2}\right]_{5/2}$ (weak), that at 14.0 nm as a blend of $4f_{7/2}^{-1}5s^2 - \left[4f_{7/2}^{-1}5s5p_{3/2}\right]_{9/2}$, $4f_{7/2}^{-1}5s^2 - \left[4f_{7/2}^{-1}5s5p_{3/2}\right]_{5/2}$, and $4f_{5/2}^{-1}5s^2 - \left[4f_{5/2}^{-1}5s5p_{3/2}\right]_{7/2}$ (weak), that at 25.7 nm as a blend of $4f_{7/2}^{-1}5s^2 - \left[4f_{7/2}^{-1}5s5p_{1/2}\right]_{5/2}$ and $4f_{5/2}^{-1}5s^2 - \left[4f_{5/2}^{-1}5s5p_{1/2}\right]_{7/2}$(weak), that at 25.9 nm as $4f_{7/2}^{-1}5s^2 - \left[4f_{7/2}^{-1}5s5p_{1/2}\right]_{9/2}$, and that at 26.0 nm as $4f_{7/2}^{-1}5s^2 - \left[4f_{7/2}^{-1}5s5p_{1/2}\right]_{7/2}$. The two Sm-like lines at 14.3 and 26.2 nm are identified as $5s^2 - \left[5s5p_{3/2}\right]_1$ and $5s^2 - \left[5s5p_{1/2}\right]_1$, respectively. The $5s - 5p$ resonance lines of the Pm-like Bi^{22+} can also be seen faintly in the calculated spectrum.

Since electron densities in CoBIT (10^{10} cm^{-3}) are relatively low, electron collision excitation and subsequent radiative decay play primary roles to determine the equilibrium populations of excited levels. Figure 2 shows the energy level diagram of the Pm-like Bi^{22+} illustrating population flows from the ground-state ($4f^{14}5s$) to the meta-stable excited-state ($4f^{13}5s^2$). Population in the ground-state can be excited to either $4f^{14}$ core states or $4f^{13}$ core states. Populations in the $4f^{14}$ core states are radiatively decayed back to the ground-state emitting the $5s - 5p$ resonance lines. On the other hand, the radiative decay from the $4f^{13}$ core states to the ground-state has small branching ratios because there is a much larger number of allowed transitions in the $4f^{13}$ core states. Most of the $4f^{13}$ core state populations radiatively cascade down into the lowest level (the lowest excited level), $4f_{7/2}^{-1}5s^2$, which is a long-lived meta-stable state and decays only via the electric octupole (E3) transition (life-time $\tau \sim 64$ s, present calculation). Table I shows population rates and equilibrium populations for $4f^{14}5s$ and $4f_{7/2}^{-1}5s^2$ states obtained by solving Eq. (1) at the electron beam energy 640 eV and the density 10^{10} cm^{-3}. The radiative in-flow rate ($\sum_{j>i} A_{ij}n_j$) to $4f_{7/2}^{-1}5s^2$ is an order of magnitude larger than that of $4f^{14}5s$. The in-flow rate to $4f_{7/2}^{-1}5s^2$ is almost balanced with the

(de)excitation rate from $4f_{7/2}^{-1}5s^2$. On the other hand, the in-flow rate to $4f^{14}5s$ is much less than the excitation rate from $4f^{14}5s$. As a result, the equilibrium population of $4f_{7/2}^{-1}5s^2$ is 14.5 times larger than that of the ground-state. Thus, the Pm-like Bi^{22+} ions in CoBIT exhibit prominent emission lines of the $4f^{13}5s^2 - 4f^{13}5s5p$ transitions, while the $5s - 5p$ resonance lines have extremely small intensities.

Radiative and dielectronic recombination rates from $4f^{14}5s$ of Bi^{22+} are calculated using the HULLAC code in order to evaluate influences from these processes. The radiative recombination rates at 640 eV are about 0.1 s^{-1}, which is three orders of magnitude smaller than the collisional excitation rate (166 s^{-1}). The present calculation predicts that dielectronic recombination via $4p^{-1}5s5l5l'$ autoionizing states of Bi^{21+} will have resonances near 640 eV. The dielectronic recombination rates at the resonances, however, are two orders of magnitude smaller than the collisional excitation rate. Charge exchange collision with neutral gas particles is roughly estimated to have a rate of 0.01 s^{-1} at most due to an extremely low pressure (10^{-7} Pa) in CoBIT. Thus, these atomic processes should not be important under the conditions of the present experiments.

Table II shows the population rates for $\left[5s5p_{1/2}\right]_0$ of the Sm-like Bi^{21+} for the electron energy 580 eV and the density 10^{10} cm^{-3}. This state has the lowest excited level which is strictly forbidden to decay to the ground-state $5s^2$ $\left({}^1S_0\right)$ by single photon emission. However, the population trapping is not facilitated for this meta-stable state because the in-flow rate is much less than the (de)excitation rate. The ${}^1S_0$ ground-state has the dominant fractional population giving prominent resonance lines due to the $5s^2 - 5s5p$ transitions (see Fig. 1).

Figure 3 shows calculated EUV spectra of the Pm-like sequence for $Z = 75 - 79$. The structures of the spectra are similar for all of the cases, but splitting of the lines *a*, *c*, and *e* and that of the lines *b* and *d* become more apparent as *Z* decreases. The present results are consistent with the measurements reported by Bekker et al. [15] and Kobayashi et al. [16]. It is noted that the cross-over of $4f^{13}5s^2$ and $4f^{14}5s$ levels occurs between Pt^{17+} and Ir^{16+} as

predicted by the previous studies [2-4]. However, calculated spectra for the Pm-like W^{13+} are hardly reconciled with the measurement as shown in Fig. 4. The term for the lowest level of $4f^{12}$ core is $\left[4f_{7/2}^{-2}5s^2 5p_{1/2}\right]_{11/2}$, which exists just above the ground-state $4f_{7/2}^{-1}5s^2$. This level is a meta-stable state which can decay via the electric-quadruple transition (A value is 0.618 s^{-1}, the present calculation). The calculation using the typical electron density in CoBIT, i.e., 10^{10} cm^{-3}, predicts a larger fractional population in the meta-stable state than that in the ground-state. Besides the emission lines associated with the $4f^{13}$ core states due to $4f^{13}5s^2 - 4f^{13}5s5p$ transitions (indicated by labels a – e) and $4f^{13}5s5p - 4f^{13}5s5d$ transitions, quite a few strong emission lines due to $4f^{12}5s^2 5p - 4f^{12}5s5p^2/5s^2 5d$ transitions (indicated by bars in the bottom figure) are seen which, however, are not apparent in the CoBIT spectrum. Thus, we identify the emission lines *a*, *b*, *c*, and *e* in the measured spectrum as the $4f^{13}5s^2 - 4f^{13}5s5p$ transitions. Calculated spectra for extremely lower electron densities show suppression of the $4f^{12}$ transitions, while intensities of the line *c* become much smaller than the measurement. Figure 5 shows the calculated wavelengths of the lines a and b and the line due to $4f^{13}5s5p - 4f^{13}5s5d$ transitions from tungsten to bismuth and comparison with the experimental values. The deviation of the wavelengths is less than 2 %.

Table III is a list for present calculations of wavelengths and transition probabilities of the $5s - 5p$ resonance lines. The wavelengths of $5s - 5p_{3/2}$ are compared with other theoretical and experimental values in Fig. 6. The experimental values are from measurements using EBITs [7, 15, 16] except for Pb^{21+}, which is measured in a beam-foil experiment [7]. Differences fall within 0.2 nm for all the elements of $Z > 77$. However, the present calculations predict a significantly shorter wavelength for Os^{15+} than the other theories and the experiment. All of the experimental wavelengths have longer values than the present calculations except for Pb^{21+}. The resonance line of W^{13+} has tentatively been identified in spectra measured at Berlin-EBIT [7, 8]. However, we exclude the data from the present

comparison because the identification in [7, 8] is controversial [17, 20]. Kobayashi et al. [15] reported that the corresponding line was not observed in the predicted region measured by CoBIT. The present calculations also predict vanishingly small fractional populations in the $4f^{14}5s$ state for the Pm-like W^{13+} (~10^{-6}) and the emission line due to the $5s - 5p_{3/2}$ transition is not apparent in the calculated spectra (Fig. 4).

4. Summary

Although Pm-like ions of $Z > 77$ have the alkaline metal-like ground-state $4f^{14}5s$, the $5s - 5p$ resonance lines are negligibly weak due to population trapping in the long-lived meta-stable excited-state $4f_{7/2}^{-1}5s^2$. The emission lines due to $4f^{13}5s^2 - 4f^{13}5s5p$ transitions are, therefore, dominant in the Pm-like spectra. The population trapping is ascribed to a large radiative in-flow rate to the $4f_{7/2}^{-1}5s^2$ state balanced with the collisional (de)excitation rate of the meta-stable state. However, the population trapping is not facilitated for the meta-stable excited-state $\left[5s5p_{1/2}\right]_0$ of Sm-like ions because the in-flow rate to this excited-state is much less than the collisional (de)excitation rate. Since the ground-state $5s^2$ has the dominant fractional population, the emission lines due to $5s^2 - 5s5p$ transitions are prominent in the Sm-like spectra.

Calculated Pm-like spectra from Bi^{22+} through W^{13+} show the similar structure, although the cross-over of $4f^{13}5s^2$ and $4f^{14}5s$ levels occurs between Pt^{17+} and Ir^{16+} as predicted by previous theoretical studies [2–4]. The present calculations are in good agreement with available measurements for all the elements with the exception of the Pm-like W^{13+}. Theoretical wavelengths of emission lines due to $4f^{13}5s^2 - 4f^{13}5s5p$ and $4f^{13}5s5p - 4f^{13}5s5d$ transitions agree with the measurements within 2 %.

Available wavelength data for the $5s - 5p_{3/2}$ resonance line are compared with the present calculations. The present calculations agree with the measurements within 0.2 nm except for Os^{15+}. The experimental wavelengths measured by EBITs [14–15] have

systematically longer values than the present calculations but for Pb^{21+} which is measured in a beam-foil experiment [7]. The present calculations predict the vanishingly small fractional abundance of $4f^{14}5s$ state for W^{13+} and the resonance line is invisible in the calculated emission spectra of W^{13+} ions in EBITs.

Acknowledgments

This work was performed with the support and under the auspices of JSPS KAKENHI Grants No. 16H04028 and No. 15H04235, and partly supported by the JSPS-NRF-NSFC A3 Foresight Program in the field of Plasma Physics (NSFC: No.11261140328, NRF: 2012K2A2A6000443).

References

1. L. J. Curtis and D. G. Ellis, Phys. Rev. Lett. 45 (1980) 2099.
2. C.E. Theodosiou and V. Raftopoulos, Phys. Rev. A 28 (1983) 1186.
3. M.J. Vilkas, Y. Ishikawa, and E. Träbert, Phys. Rev. A 77 (2008) 042510.
4. U.I. Safronova, A.S. Safronova, and P. Beiersdorfer, Phys. Rev. A 88 (2013) 032512.
5. B. M. Johnson, K.W. Jones, T. H. Kruse, L. J. Curtis, and D. G. Ellis, Nucl. Instrum. Methods 202 (1982) 53.
6. E. Träbert and P. H. Heckmann, Z. Phys. D 1 (1986) 381.
7. R. Hutton, Y. Zou, J. R. Almandos, C. Biederman, R. Radtke, A. Greier, and R. Neu, Nucl. Instrum. Methods B 205 (2003) 114.
8. S. Wu and R. Hutton, Can. J. Phys. 86 (2008) 125.
9. K. B. Fournier, M. Finkenthal, S. Lippmann, C. P. Holmes, H. W. Moos, W. H. Goldstein, and A. L. Osterheld, Phys. Rev. A 50 (1994) 3727.
10. O. Andersson, A Method for Atomic Spectroscopy of Highly Charged Ions in the Pm Isoelectronic Sequence, Master's thesis, Lund University, 1995.

11. E. Träbert, M. J. Vilkas, and Y. Ishikawa, J. Phys.: Conf. Ser. 163 (2009) 012017.

12. V. Jonauskas, Š. Masys, A. Kynienė, and G. Gaigalas, J. Quant. Spectrosc. Radiat. Transfer 127 (2013) 64.

13. Y. Kobayashi, D. Kato et al, Phys. Rev. A 89 (2014) 010501(R).

14. N. Nakamura, H. Kikuchi, H. A. Sakaue, and T. Watanabe, Rev. Sci. Instrum. 79 (2008) 063104.

15. H. Bekker et al., J. Phys. B: At. Mol. Opt. Phys. 48 (2015) 144018.

16. Y. Kobayashi et al, Phys. Rev. A 92 (2015) 022510.

17. W. Li et al., Phys. Rev. A 91 (2015) 062501.

18. A. Bar-Shalom, M. Klapisch, and J. Oreg, J. Quant. Spectrosc. Radiat. Trans. 71 (2001) 169.

19. T. A. Carlson, C. W. Nestor, Jr., N. Wasserman, and J. D. McDowell, At. Data Nucl. Data Tables 2 (1970) 63.

20. A. Kramida, Can. J. Phys. 89 (2011) 551.

Table I: Breakdown of population rates (s^{-1}) for the ground-state $4f^{14}5s$ and meta-stable excited-state $4f_{7/2}^{-1}5s^2$ of Pm-like Bi^{22+} ions in CoBIT. The second and third columns are in-flow rates to these states due to collisional (de)excitation ($n_e \sum_{j\neq i} C_{ij} n_j$) and radiative cascade ($\sum_{j>i} A_{ij} n_j$), respectively. The fourth and fifth columns are collisional (de)excitation rates ($n_e \sum_{j\neq i} C_{ji}$) and radiative decay rates ($\sum_{j<i} A_{ji}$) from these states, respectively. The sixth and seventh columns are the fractional populations (n_i) and the relative populations to the ground-state, respectively. The present results are obtained at the electron beam energy 640 eV and the density 10^{10} cm^{-3}.

	In-col (s^{-1})	In-rad (s^{-1})	Out-col (s^{-1})	Out-rad (s^{-1})	n_i	Relative population
$4f^{14}5s$ (ground)	0.054	10.6	166	0	0.064	1
$4f_{7/2}^{-1}5s^2$ (meta-stable)	0.021	200	216	0.016	0.928	14.5

Table II: Breakdown of population rates (s^{-1}) for the meta-stable excited-state $\left[5s5p_{1/2}\right]_0$ of Sm-like Bi^{21+} ions in CoBIT. Same as Table I.

	In-col (s^{-1})	In-rad (s^{-1})	Out-col (s^{-1})	Out-rad (s^{-1})	n_i	Relative population
$\left[5s5p_{1/2}\right]_0$ (meta-stable)	0.03	5.25	123	0	0.043	0.048

Table III: Calculated wavelengths (λ) and transition probabilities (A) of the $5s - 5p$ resonance lines. Numbers in parentheses stand for exponents of 10^x, i.e., $a(x) = a \times 10^x$

	$5s - 5p_{1/2}$		$5s - 5p_{3/2}$	
	λ (nm)	A (s^{-1})	λ (nm)	A (s^{-1})
W^{13+}	36.508	1.10(10)	26.026	2.99(10)
Re^{14+}	34.614	1.23(10)	24.176	3.59(10)
Os^{15+}	32.689	1.15(10)	22.271	3.61(10)
Ir^{16+}	32.018	9.47(9)	21.236	4.49(10)
Pt^{17+}	30.175	1.60(10)	19.811	5.74(10)
Au^{18+}	28.752	1.77(10)	18.530	6.70(10)
Pb^{21+}	25.332	2.23(10)	15.358	1.02(11)
Bi^{22+}	24.320	2.39(10)	14.446	1.16(11)
U^{31+}	17.781	4.05(10)	8.676	3.57(11)

List of figure captions

Fig. 1: Emission line spectra of Pm-like and Sm-like bismuth ions in CoBIT (above) measured at three electron beam energies and calculated spectra (below) at 580 eV (Sm-like) and 640 eV (Pm-like) for the electron density of 10^{10} cm^{-3}. The calculated spectra are convoluted with Gaussian distribution functions having a full-width at half-maximum of 0.03 nm.

Fig. 2: Energy level diagram of Pm-like bismuth. Excitation rates (s^{-1}) from the ground-state ($4f^{14}5s$) to $4f^{14}5p_{1/2}$ and $4f^{14}5p_{3/2}$, and the total excitation rate to $4f^{13}5s\{5p, 5d, 5f, 5g, 6s, 6p, 6d, 6f, 6g\}$ at n_e = 10^{10} cm^{-3} are also indicated.

Fig .3: Calculated EUV spectra of the Pm-like sequence for elements of $Z = 75 - 79$. Electron beam energies used in the calculations are 480, 440, 400, 360, and 330 eV for Au^{18+}, Pt^{17+}, Ir^{16+}, Os^{15+}, and Re^{14+}, respectively. The electron density is 10^{10} cm^{-3}. The calculated spectra are convoluted with Gaussian distribution functions having a full-width at half-maximum of 0.03 nm.

Fig. 4: CoBIT measurement vs calculations for the EUV spectrum of the Pm-like W^{13+}. The top figure is the measurement. The calculated spectra at 300 eV are shown in four figures from the bottom for four different electron densities from 10^{10} cm^{-3} down to 10^{7} cm^{-3} assumed in the calculations, respectively. Labels of emission lines are the same as in Fig. 3. Bars in the bottom figure indicate emission lines due to the $4f^{12}5s^25p - 4f^{12}5s5p^2/5s^25d$ transitions. The wavelength scale of the calculated spectra is shifted by +0.43 nm.

Fig. 5: Calculated wavelengths of Pm-like lines ($\lambda_{\mathrm{HULLAC}}$) and comparison with available experimental values: [15] for W^{13+}, Au^{18+}, and Bi^{22+}, and [14] for the others.

Fig. 6: Comparison of theoretical and experimental wavelengths of the $5s - 5p_{3/2}$ resonance line. Deviation (nm) from the present calculations using HULLAC code is plotted. The experimental wavelength values are indicated in the figure (nm): [7] for Pb^{21+}, [14] for Re^{14+}, Os^{15+}, Ir^{16+}, and Pt^{17+}, and [15] for Au^{18+} and Bi^{22+} (tentative). Other theoretical results are obtained by multi-reference Møller-Plesset method (MR-MP) [3], configuration interaction using Dirac-Fock-Sturmian basis (CIDFS) [14], flexible atomic code (FAC) [14], relativistic many-body perturbation with Breit-Dirac-Fock potential (RMBPTB) [4], and the Cowan code [4].

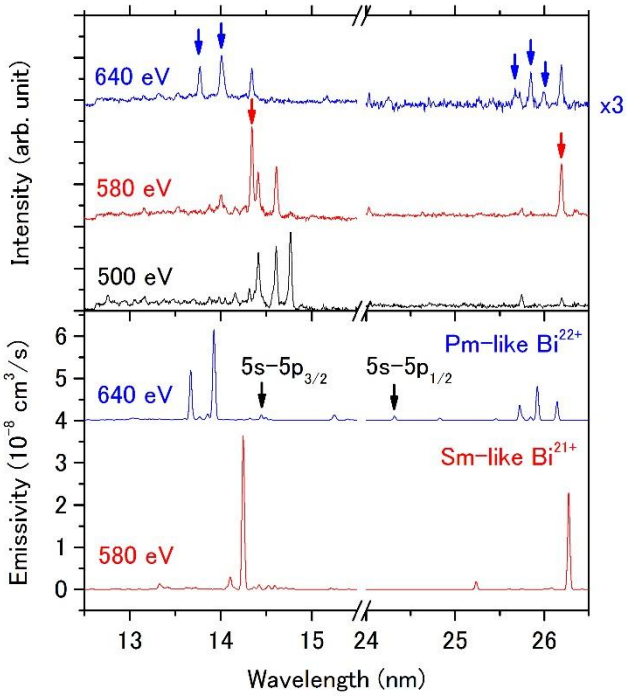

Figure 1

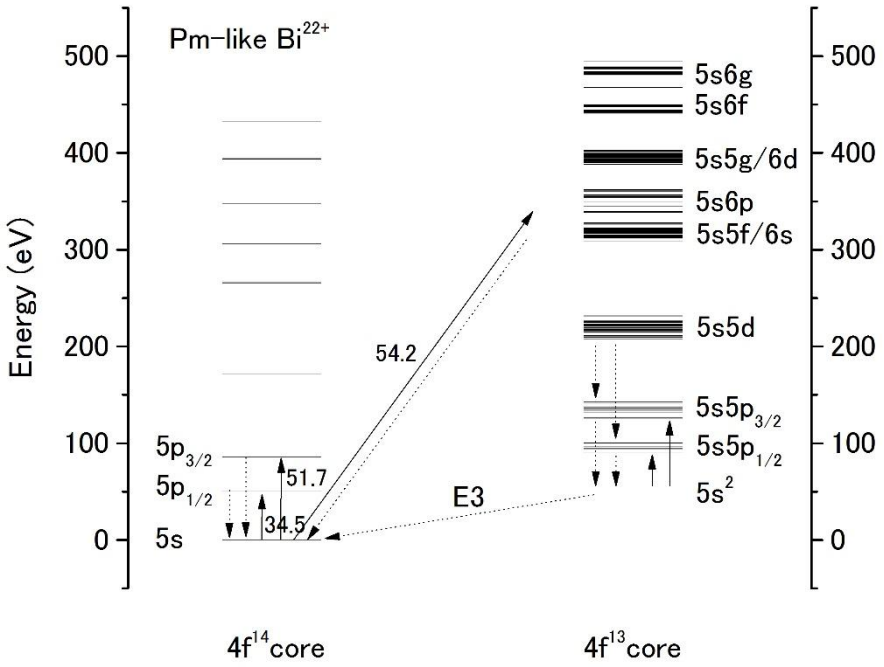

Figure 2

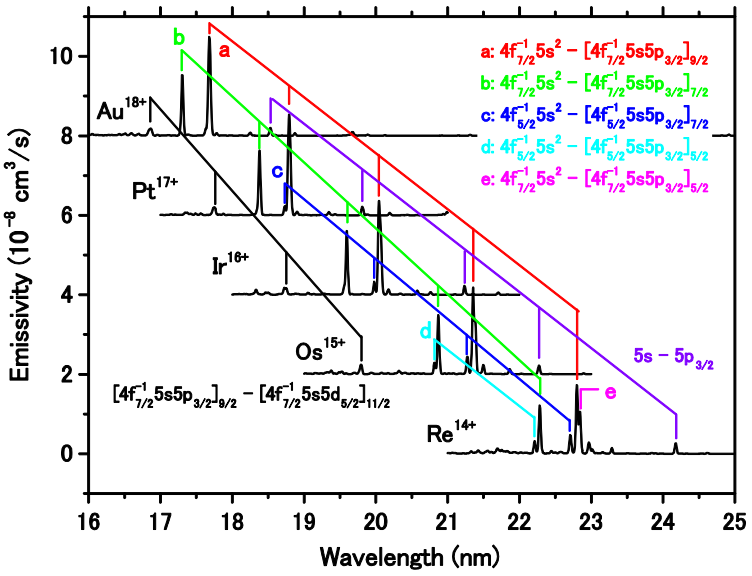

Figure 3

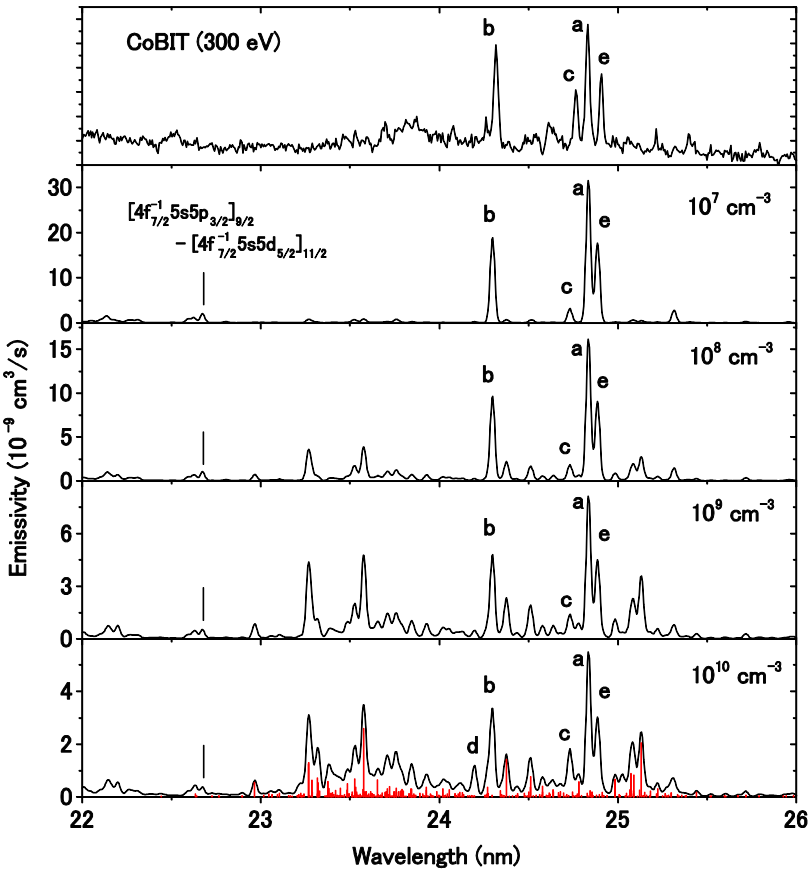

Figure 4

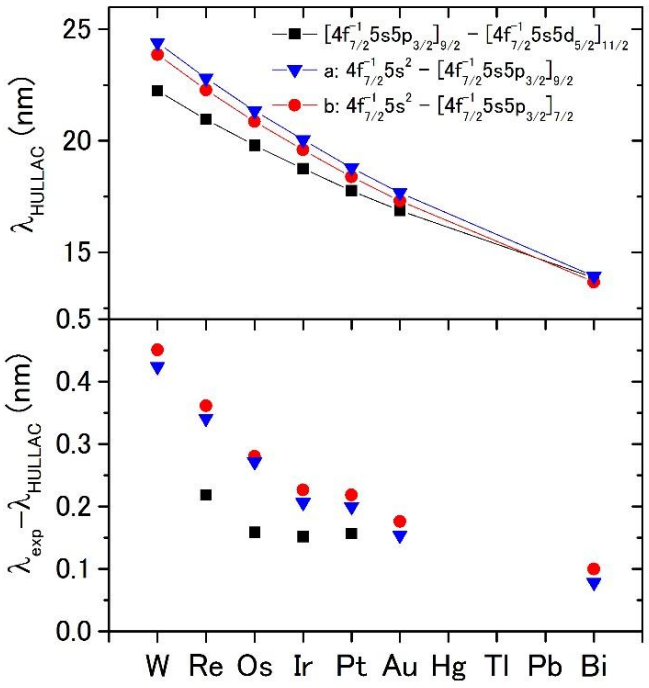

Figure 5

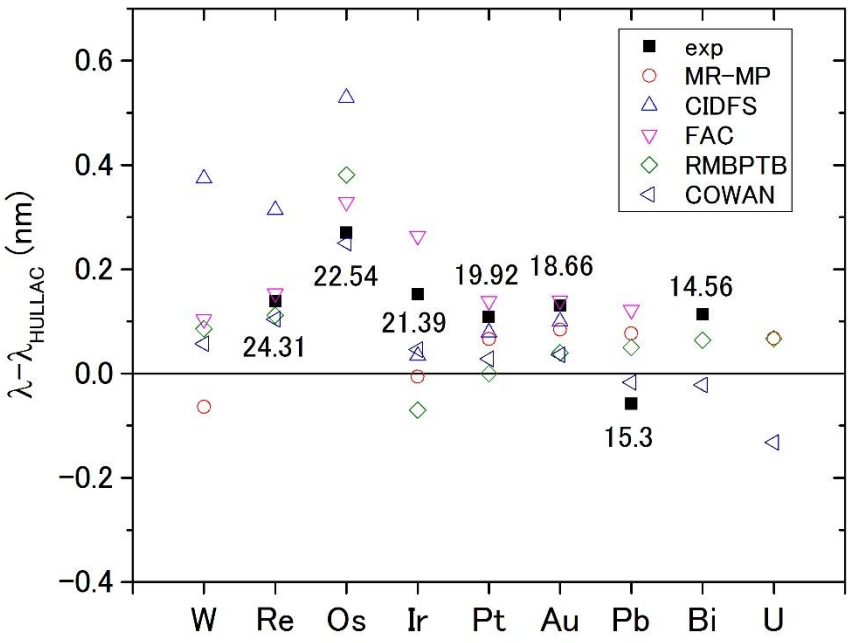

Figure 6